



Published in final edited form as:

Magn Reson Imaging. 2007 September ; 25(7): 1032–1038.

A Practical Guide to Robust Detection of GABA in Human Brain by J-difference Spectroscopy at 3 Tesla Using a Standard Volume Coil

Kevin W. Waddell^{1,2}, Malcolm J. Avison^{1,2,3,4}, James M. Joers^{1,2}, and John C. Gore^{1,2,5,6,7}

¹*Institute of Imaging Science, Vanderbilt University, Nashville, Tennessee, 37232-2675*

²*Department of Radiology and Radiological Sciences, Vanderbilt University, Nashville, Tennessee, 37232-2675*

³*Department of Neurology, Vanderbilt University, Nashville, Tennessee, 37232-2675*

⁴*Department of Pharmacology, Vanderbilt University, Nashville, Tennessee, 37232-2675*

⁵*Department of Molecular Physiology and Biophysics, Vanderbilt University, Nashville, Tennessee, 37232-2675*

⁶*Department of Biomedical Engineering, Vanderbilt University, Nashville, Tennessee, 37232-2675*

⁷*Department of Physics, Vanderbilt University, Nashville, Tennessee, 37232-2675*

Abstract

γ -Aminobutyric acid (GABA) is the major inhibitory neurotransmitter in human brain and has been implicated in several neuropsychiatric disorders. In-vivo human brain GABA concentrations are near the detection limit for magnetic resonance spectroscopy (~ 1 mM) and because of overlap with more abundant compounds, spectral editing is generally necessary to detect GABA. In previous reports, GABA spectra edited by J-difference spectroscopy vary considerably in appearance. We have evaluated the factors that affect GABA spectra and the conditions necessary for robust acquisition of J-difference spectra from arbitrary brain regions. In particular, we demonstrate that variations in spectral quality can be explained in part by the incoherent addition of transients that results from shot to shot frequency and phase variations. An automated time-domain spectral alignment strategy is presented that enables reproducible acquisition of high-quality GABA spectra at 3 Tesla with a standard 30 cm T/R volume coil. Representative GABA spectra from human frontal lobe, an area where susceptibility-induced frequency and phase variations are especially troublesome, are presented that demonstrate the robustness of the acquisition and data handling strategy used in this study.

Keywords

GABA; editing; difference spectroscopy; MEGA-PRESS; frequency variations; phase variations; susceptibility effects; in-vivo magnetic resonance spectroscopy; frontal lobe

Address correspondence to: Kevin W. Waddell, Ph.D., Institute of Imaging Science, Vanderbilt University, 1161 21st Avenue South, MCN AA 1105, Nashville, Tennessee 37232-2310.

Publisher's Disclaimer: This is a PDF file of an unedited manuscript that has been accepted for publication. As a service to our customers we are providing this early version of the manuscript. The manuscript will undergo copyediting, typesetting, and review of the resulting proof before it is published in its final citable form. Please note that during the production process errors may be discovered which could affect the content, and all legal disclaimers that apply to the journal pertain.

1. Introduction

γ -Aminobutyric acid (GABA) is the major inhibitory neurotransmitter in the brain [1], and altered GABA levels and/or GABA turnover rates have been implicated in a range of neurological and psychiatric disorders [2-6]. At a concentration of ~ 1 mM in cortical grey matter (GM) in humans, GABA lies within the sensitivity limits of standard clinical 3T MR scanners. However, the routine detection and robust quantification of GABA *in vivo* are complicated by the presence of co-resonant metabolite peaks, including creatine (3.03 ppm), so-called macromolecule resonances (3.0 ppm) [7] and homocarnosine, a dipeptide formed from GABA and histidine [8]. As a result, GABA is completely obscured by creatine at field strengths and spectral resolutions typical of human MRS, and additional experiments are generally necessary to estimate the contribution of co-edited homocarnosine and macromolecules. Thus direct quantification of GABA is generally not feasible. To address this, a variety of strategies have been described for selectively editing the GABA resonance from the complicated spectral background. These methods generally exploit the J-coupling of the GABA C-4 resonance of interest at 3.01 ppm [9] to the GABA C-3 protons at 1.91 ppm (see Figure 1), using J-difference editing [10-13] or multiple quantum filters [14-17]. J-difference editing is conceptually simpler and generally more sensitive than MQF, but requires 2 sets of experiments. Hence, J-difference spectroscopy is inherently more sensitive to experimental factors such as instrument instability or physiologically induced frequency and phase variations than single shot methods. Moreover, these experimental imperfections result in cumulative errors that diminish the advantage of coherent averaging. These effects are especially acute for studies requiring volume coils (outside occipital lobe), where larger numbers of acquisitions are necessary to compensate for a lack of sensitivity relative to studies using surface coils. Even with surface coils, studies typically require hundreds of acquisitions. This paper outlines the practical requirements for implementing clinically robust GABA* (GABA + macromolecules + homocarnosine) detection using a standard volume coil by J-difference spectroscopy at 3 Tesla.

In particular, we demonstrate the essential strategies required for reproducible acquisition of high-quality data consistent with known features of the GABA spin-system from a standard 3T research scanner. In addition to the needs of accurate timing and adequate crusher gradient areas, the importance of acquiring independent phase-cycled shots and implementing an automatic post-processing strategy to minimize the impact of frequency and phase variations is illustrated. It is shown that some of the broad component at 3.01 ppm that is typically attributed to co-edited macromolecules is suppressed with this approach, suggesting that this contamination is partly an avoidable consequence of incoherent averaging.

2. Theory

The RF portion of the MEGA-PRESS [11,18] pulse sequence is:

$$\left(\frac{\pi}{2}\right)_x^{ss} - \tau_1 - (\pi)_x^{ss} - \tau_2 - (\pi)_x^{si} - \tau_3 - (\pi)_x^{ss} - \tau_4 - (\pi)_x^{si} - \tau_5 - (\text{acq}), \quad (1)$$

where the superscripts “ss” and “si” denote slice-selective and selective inversion, respectively (see Figure 2). The timing constraints required for nulling J-evolution are reviewed using an abbreviated product operator analysis for a coupled two spin system. Starting with an equilibrium density operator proportional to I_z and using the convention that a positive rotation about the x-axis will transform I_z to $-I_y$, the effect of the MEGA-PRESS sequence is:

$$I_z \rightarrow -I_y \cos(\pi J_{IS} (\tau_1 + \tau_2 - \tau_3 - \tau_4 + \tau_5)) + 2I_x S_z \sin(\pi J_{IS} (\tau_1 + \tau_2 - \tau_3 - \tau_4 + \tau_5)), \quad (2)$$

where the analogous expression for the S spin has been omitted. Therefore, when

$$\tau_1 + \tau_2 + \tau_5 = \tau_3 + \tau_4, \quad (3)$$

the resulting signal is time-independent, absorptive, and in phase with the excitation pulse. The interval τ_1 depends on the durations of the excitation pulse, rephasing and crusher gradients, as well as of the first slice-selective refocusing pulse, and this interval is usually made as small as possible. As an additional constraint, the effects of frequency offsets should also be refocused resulting in the following timing conditions:

$$\begin{aligned} \tau_1 &= \text{shortest} \\ \tau_2 &= TE / 4 \\ \tau_4 &= TE / 4 \\ \tau_5 &= TE / 2 - \tau_1 - \tau_2 \\ \tau_3 &= TE / 2 - \tau_4 \end{aligned} \quad (5)$$

The second set of crusher gradients are also rearranged in the MEGA-PRESS [11,18] sequence. This rearrangement has the effect of dephasing resonances that experience selective inversion. As pointed out in the original references, this affords robust water suppression when an additional inversion band is added to the selective pulses and has the additional practical advantage of dephasing the inverted NAA resonance, which would otherwise lead to a much larger baseline dip after differencing.

3. Methods

3.1. Spectroscopy

20 normal volunteers were studied in accordance with procedures approved by the Vanderbilt University Institutional Review Board. All experiments were performed on a 3 Tesla Philips Achieva spectrometer (release 1.2.2) with the standard T/R 30.0 cm diameter volume coil and the radio frequency pulse library supplied by the manufacturer as part of their standard system. Side to side head movements were minimized by placing foams pads between the volunteers' ears and the volume coil. GABA data were acquired using the MEGA-PRESS pulse sequence [11,18] from 15-40 mL volumes (99% coverage) with echo times of 70 ms and recycle delays of 2.5 seconds. Note that Philips uses 99% coverage to define pulse bandwidths in contrast to full width at half maximum (fwhm). Consequently, for the slice-select pulses employed here, volumes defined by fwhm are 2.46 times smaller. Hence, stated volumes should be divided by 2.46 for sensitivity comparisons to other vendors that use the fwhm pulse bandwidth definition. 2000 complex points were sampled and the receiver bandwidth was 2 kHz. Prior to FFT, J-difference time-domain spectra were apodized with a 4 Hz exponential function. Crusher gradients magnitudes were maintained nominally at > 20 mT/m, but the actual values varied somewhat due to a recalculation designed to minimize eddy currents. Selective inversions were achieved with 15.64 ms sinc-center pulses (64 Hz bandwidth), and these were applied at the 1.91 ppm C-3 resonance of GABA on odd numbered acquisitions and at a position symmetric about the water resonance on even numbered acquisitions in order to reduce baseline artifacts. With these pulse characteristics, the effect of differential response on the integrated area at 3.0 ppm was estimated to be less than 0.1% from simulations written in C++ using the GAMMA libraries [19]. The carrier frequency was maintained within ~2 Hz using the manufacturer $^1\text{H}_2\text{O}$ navigator based frequency drift compensation option. A sinc-gauss CHES water suppression pulse [20] with a refocusing bandwidth of 140 Hz preceded localization. RF power and shim settings (second order) were optimized on voxels of interest using the standard Philips spectroscopy preparation routine. To facilitate retrospective

frequency and phase corrections, the standard release Philips pulse sequences were modified to allow acquisition and storage of phase-cycled single shots.

3.2. Post-processing

The experimental arrays of frequency toggled (odd/even scans) and phase-cycled free induction decays (fids) were processed automatically using a 2 step algorithm to remove phase and frequency variations. In the first step, the creatine resonance of the summed fid was fit to the real part of a lorentzian using global nonlinear least squares with a phase and frequency search radius of 360 degrees and 12 Hz, respectively, and first guesses for the amplitude and linewidth were generated from the averaged frequency domain spectrum. In step 2, each fid was fit using these first guesses, albeit with the amplitude divided by the number of transients, in a more tightly constrained but otherwise identical time-domain fitting procedure. The success of this spectrally navigated time-domain nonlinear least squares procedure depends on the signal to noise ratio (SNR) available in each shot and, when used on voxel volumes typical of GABA experiments (15-40 mL), this automatic procedure has proven reliable as judged by convergence and improved SNR across the spectrum. The SNR threshold for robust convergence could be lowered further by exploiting additional prior knowledge in the fitting step, such as the choline singlet. The accuracy of quantitative measurements was improved by discarding those transients (and the corresponding frequency toggled counterparts) whose fit parameters (amplitude, zeroth order phase, frequency, linewidth) deviated more than 3 standard deviations from the respective mean; this statistical threshold typically resulted in the removal of 5-10 "corrupt" acquisitions and eliminated the need for baseline fitting prior to integration of the GABA pseudo-doublet at 3.01 ppm.

4. Results

As a practical guide to using this method, the key elements of implementing MEGA-PRESS on a standard clinical 3T scanner are summarized below. Starting from a PRESS template, two rf waveforms must be added with the timing constraints discussed earlier and with the crusher gradients rearranged as discussed in the original reference, a real-time variable must be used to toggle the frequencies of the added inversion pulses using an available real-time loop, and the method of data acquisition/storage must be modified to enable collection of phase-cycled single shots. In our experience, the latter modification is critical for reproducible acquisition of data with the expected lineshape and an observable splitting consistent with the GABA spin-system [9]. In implementing the sequences, data from a phantom should first be analyzed, preferably from a single phase cycle to eliminate the cumulative impacts of spectrometer instability, to verify that the 1.91 ppm resonance is inverted and dephased on alternate acquisitions, and that the edited doublet at 3.01 ppm is consistent with a full density matrix simulation in appearance and editing efficiency.

The GABA spin-system (excluding amino protons) is illustrated in Figure 1; chemical shifts and J-coupling constants of indexed protons are described in Table 1. Simulated and experimental GABA J-difference edited spectra are shown in Figure 3 from a phantom containing a 10:1 mixture of creatine and GABA. In this figure, the bottom trace results from simulating the GABA spin-system as an $A_2X_2W_2$ spin-system, an approximation to the true $AA'XX'WW'$ spin-system [9]. That is, GABA has three pairs of protons (not counting unobserved carboxyl and amine protons) corresponding to three chemical shifts, but J-couplings between each proton within a pair to their analogs on adjacent carbons are distinct (See Table 1). The phantom (top trace) and the $AA'XX'WW'$ simulation (middle trace) are in excellent agreement aside from a slight asymmetry apparent in the phantom spectrum, which arises mainly from the creatine subtraction error. By repeating the experiment on a phantom containing only creatine, the subtraction error was estimated to be 0.07 % (% of creatine

intensity). In-vitro dispersive subtraction errors are primarily a manifestation of inaccurate carrier frequency updates between acquisitions and, secondarily, could also result from time-dependent lineshape variations. In-vivo, susceptibility-induced frequency shifts also occur and these can cause phase variations when the shifts happen during the editing pulse sequence. Human brain creatine concentrations are approximately 8 $\mu\text{mol/g}$ [13] compared to a GABA concentration of $\sim 1 \mu\text{mol/g}$, and three 3.00 ppm methyl protons contribute to the creatine resonance compared to two for the 3.01 ppm GABA resonances. In addition, because the center resonance of the 3.01 ppm GABA resonances remains approximately stationary on odd and even scans, half of the available GABA sensitivity is lost upon differencing. Due to the large differences in concentration and these unfavorable characteristics of the edited GABA peak, subtraction errors should be maintained at $\sim 2\%$ or less, and these can be estimated in-vivo from the subtraction error of the 3.22 ppm choline resonance. The theoretical editing efficiency using the specified inversion pulses was 97.1%, as determined by comparing the edited area of the 3.01 ppm doublet from pulse sequence simulations employing ideal versus real inversion pulses. The experimental editing efficiency ($\sim 96\%$) was estimated by dividing the wing resonance magnitudes from odd acquisitions (inversion “on”) to twice the wing resonance magnitudes from the even acquisitions (inversion “off”). This suggests the editing efficiency is dominated by the inversion pulse characteristics for short experiments. Deviations from the nominal editing efficiency can result from imperfect carrier frequency updates between acquisitions; these transmitter variations simultaneously reduce the inversion pulse efficiency and increase the likelihood of co-editing lysine macromolecular resonances [7] when the variations are systematically upfield. At 3 Tesla, the deleterious impact on editing efficiency as a result of shot-shot frequency and phase variations (see Figure 4) amounts to a $\sim 1\%$ underestimation of GABA concentration and changes in co-editing are largely irrelevant because variations tend to be distributed about the correct mean frequency. Under most circumstances, both of these effects are negligible, but an ancillary benefit of retrieving and storing experimental inaccuracies is that corrections can be made transparently in the course of data analysis using look-up tables (efficiency versus inversion pulse frequency and phase) based on simulations. Acquisition of phase-cycled single shots coupled with a strategy to correct for inter-acquisition frequency and phase variations is necessary to maximize SNR and resolution; this is demonstrated for a typical GABA data set in Figure 4. The chosen correction procedure is automatic, minimizing the need for tedious inspection of 500 or so data sets, as well as consistent, and the corrected data (red trace) demonstrates that the alignment is nonlocal, spanning the 0.5 ppm to 4.0 ppm range.

In the absence of spectral alignment, subtraction errors result in baseline artifacts that often overwhelm the edited GABA doublet, and the inevitable line broadening washes away the characteristic GABA splitting. The former effect results in a jagged baseline that complicates integration and impedes fit convergence while the latter will systematically increase the limits of errors in quantification due to the loss of spectral information (2 peaks versus 1). Representative human in-vivo spectra acquired from a 22.5 mL frontal voxel containing mostly grey matter that illustrates these effects are shown in Figure 5.

Corrected (top trace) and uncorrected spectra (bottom trace) are plotted on the same scale; SNR is increased in the aligned data by $\sim 10\%$ as a result of line-narrowing. Sensitivity enhancements from spectral alignment depend on the voxel placement though, and improvements in sensitivity from areas that are relatively insensitive to magnet susceptibility effects are $\sim 2\%$. Effective increases in resolution and sensitivity are also visible from the co-edited doublet at ~ 3.7 ppm, which is a combination of glutamate, glutamine and glutathione. 19 out of 20 data sets acquired from a sample of brain grey matter and post-processed as described were judged to provide acceptable GABA* spectra, as ascertained from the GABA* edited peak structure (12-14 Hz splitting) and the edited GABA* ratios with respect to creatine. The edited GABA* peak structure, characterized by reasonable intensities deemed from

creatine and GABA* intensity ratios and splittings from 12-14 Hz, is observed in 19 out of 20 data sets acquired and corrected by the process outlined. In contrast, expected GABA doublet intensity ratios and splitting were observed in only 5 out of 20 data sets where the retrospective alignment was not performed. Pathological data sets where minimal improvement is realized are rare ($\sim 1/20$) and thought to arise from the effects of bulk motion, as ascertained by analyzing the distribution of fit parameters (such as linewidth) as a function of time. Acquisition indices where fit parameters differ from the mean more than a predetermined statistical threshold (e.g. ± 3 standard deviations) can be used to define acquisitions as corrupt. Normally this criterion is satisfied by $>95\%$ of the acquisitions, but as a consequence of bulk motion the voxel is shifted to an unshimmed region. Hence, the likelihood that fit parameters such as linewidth, frequency and amplitude will stay within ± 3 standard deviations of the mean values obtained from the shimmed region decreases. In this case, the array of acquisition indices that fail to satisfy the statistical threshold will contain an abrupt transition from a sparse to a continuous distribution.

Intensity ratios of GABA* to other compounds which are present in either the odd scans, even scans, or the difference spectrum are proportional to the respective concentration ratios, and these values can be quickly determined by standard peak-picking algorithms or by visual inspection. Hence, intensity ratios listed in Table II serve as a convenient practical metric to quickly assess whether measured values seem reasonable when compared to a database of region-specific normative values in the population of interest.

5. Discussion

The proliferation of human 3 Tesla scanners equipped with volume coils, coupled with an increased interest in obtaining region specific GABA measurements for neuropsychiatric applications demands the development of robust and reliable methods for practical implementation in clinical research setting. The MEGA-PRESS [11,18] pulse sequence has been featured in numerous previous studies due to its conceptual simplicity and relative ease of implementation. Although several reports using GABA editing have appeared in the literature, data quality, as ascertained by well-behaved baselines and edited peak splittings consistent with the GABA spin-system, has varied widely. Higher quality human spectra have generally been acquired with surface coil transceivers that restrict voxel locations to parietal and occipital lobes. Volume coils at 3T are comparably less efficient than their surface coil counterparts, leading to longer acquisition times to achieve adequate SNR. As the length of acquisition increases, a robust method, such as the time-domain alignment described here, for collecting and aligning the data becomes increasingly important.

In the context of difference spectroscopy, retrospective frequency and phase alignment based on the N-acetylaspartate (NAA) peak has previously been used for the detection of glutathione [21]. The details and the effectiveness of this alignment procedure were not presented though. Thiel and coworkers [22] recently reported a retrospective alignment and rejection strategy based on spectral deconvolution with a $^1\text{H}_2\text{O}$ navigator acquired during the relaxation delay. While this was shown to improve spectral quality and should be independent of SNR ($^1\text{H}_2\text{O}$ is abundant), in circumstances where SNR is sufficient, it may be less accurate than fitting to singlet signatures in the spectrum because the navigator is sampled during an interval distinct from the acquisition of the main spectrum.

It has been demonstrated that the edited GABA* doublet is consistently observed (19/20) when phase-cycled single shots are aligned based on the singlet signatures (choline, creatine, or both). Broad featureless GABA peaks are thus not completely attributable to macromolecules, although it is generally accepted that, in the absence of additional measures to null macromolecules, GABA estimates will be overestimated by as much as a factor of 2 [7].

Strategies to eliminate contamination have been detailed in the literature and should be employed in addition to the basic ingredients reviewed here for quantitative GABA estimates [7,10,23]. The approach proposed by Henry and coworkers, whereby the inversion pulse is toggled about the upfield macromolecule resonance at 1.7 ppm, is the most time-efficient approach but requires the use of double-banded pulses to null the water resonance on each acquisition. Otherwise, the asymmetric response at the water resonance on odd versus even acquisitions will lead to large baseline artifacts [23]. Metabolite nulling based on T1 differences is also suitable and has the advantage of ease of implementation, as most standard scanners have built-in modules for T1 nulling [7], but suffers from the necessity of making assumptions about contaminant longitudinal relaxation times.

Acknowledgements

This work was supported by an NIH training grant 5T32 EB001628 entitled "Postdoctoral Training in Biomedical MRI and MRS" and an NIH Biomedical Research Partnership grant EB0000461. We thank Philips Medical Systems (Netherlands) for hardware and software support.

References

1. McCormick DA. GABA as an inhibitory neurotransmitter in human cerebral cortex. *J Neurophysiol* 1989;62:1018–27. [PubMed: 2573696]
2. Epperson CN, O'Malley S, Czarkowski KA, Gueorguieva R, Jatlow P, Sanacora G, Rothman DL, Krystal JH, Mason GF. Sex, GABA, and nicotine: the impact of smoking on cortical GABA levels across the menstrual cycle as measured with proton magnetic resonance spectroscopy. *Biol Psychiatry* 2005;57:44–8. [PubMed: 15607299]
3. Sanacora G, Gueorguieva R, Epperson CN, Wu YT, Appel M, Rothman DL, Krystal JH, Mason GF. Subtype-specific alterations of gamma-aminobutyric acid and glutamate in patients with major depression. *Arch Gen Psychiatry* 2004;61:705–13. [PubMed: 15237082]
4. Goddard AW, Mason GF, Appel M, Rothman DL, Gueorguieva R, Behar KL, Krystal JH. Impaired GABA neuronal response to acute benzodiazepine administration in panic disorder. *Am J Psychiatry* 2004;161:2186–93. [PubMed: 15569888]
5. Krystal JH, Sanacora G, Blumberg H, Anand A, Charney DS, Marek G, Epperson CN, Goddard A, Mason GF. Glutamate and GABA systems as targets for novel antidepressant and mood-stabilizing treatments. *Mol Psychiatry* 2002;7:S71–80. [PubMed: 11986998]
6. Sanacora G, Mason GF, Krystal JH. Impairment of GABAergic transmission in depression: new insights from neuroimaging studies. *Crit Rev Neurobiol* 2000;14:23–45. [PubMed: 11253954]
7. Behar KL, Rothman DL, Spencer DD, Petroff OA. Analysis of macromolecule resonances in 1H NMR spectra of human brain. *Magn Reson Med* 1994;32:294–302. [PubMed: 7984061]
8. Kish SJ, Perry TL, Hansen S. Regional distribution of homocarnosine, homocarnosine-carnosine synthetase and homocarnosinase in human brain. *J Neurochem* 1979;32:1629–36. [PubMed: 448355]
9. Govindaraju V, Young K, Maudsley AA. Proton NMR chemical shifts and coupling constants for brain metabolites. *NMR Biomed* 2000;13:129–53. [PubMed: 10861994]
10. Terpstra M, Ugurbil K, Gruetter R. Direct in vivo measurement of human cerebral GABA concentration using MEGA-editing at 7 Tesla. *Magn Reson Med* 2002;47:1009–12. [PubMed: 11979581]
11. Mescher M, Merkle H, Kirsch J, Garwood M, Gruetter R. Simultaneous in vivo spectral editing and water suppression. *NMR Biomed* 1998;11:266–72. [PubMed: 9802468]
12. Hetherington HP, Newcomer BR, Pan JW. Measurements of human cerebral GABA at 4.1 T using numerically optimized editing pulses. *Magn Reson Med* 1998;39:6–10. [PubMed: 9438430]
13. Rothman DL, Petroff OA, Behar KL, Mattson RH. Localized 1H NMR measurements of gamma-aminobutyric acid in human brain in vivo. *Proc Natl Acad Sci U S A* 1993;90:5662–6. [PubMed: 8516315]
14. Choi IY, Lee SP, Merkle H, Shen J. Single-shot two-echo technique for simultaneous measurement of GABA and creatine in the human brain in vivo. *Magn Reson Med* 2004;51:1115–21. [PubMed: 15170830]

15. Shen J, Rothman DL, Brown P. In vivo GABA editing using a novel doubly selective multiple quantum filter. *Magn Reson Med* 2002;47:447–54. [PubMed: 11870830]
16. Shen J, Shungu DC, Rothman DL. In vivo chemical shift imaging of gamma-aminobutyric acid in the human brain. *Magn Reson Med* 1999;41:35–42. [PubMed: 10025609]
17. Wilman AH, Allen PS. Yield enhancement of a double-quantum filter sequence designed for the edited detection of GABA. *J Magn Reson B* 1995;109:169–74. [PubMed: 7582599]
18. Mescher M, Tannus A, ONJ M, Garwood M. Solvent Suppression using Selective Echo Dephasing. *J Magn Reson A* 1996;123:226–229.
19. Smith SA, Levante TO, Meier BH, Ernst R. Computer simulations in magnetic resonance. An object oriented programming approach. *J Magn Reson A* 1994;106:75–105.
20. Haase A, Frahm J, Hanicke W, Matthaei D. 1H NMR chemical shift selective (CHESS) imaging. *Phys Med Biol* 1985;30:341–4. [PubMed: 4001160]
21. Terpstra M, Henry PG, Gruetter R. Measurement of reduced glutathione (GSH) in human brain using LCModel analysis of difference-edited spectra. *Magn Reson Med* 2003;50:19–23. [PubMed: 12815674]
22. Thiel T, Czisch M, Elbel GK, Hennig J. Phase coherent averaging in magnetic resonance spectroscopy using interleaved navigator scans: compensation of motion artifacts and magnetic field instabilities. *Magn Reson Med* 2002;47:1077–82. [PubMed: 12111954]
23. Henry PG, Dautry C, Hantraye P, Bloch G. Brain GABA editing without macromolecule contamination. *Magn Reson Med* 2001;45:517–20. [PubMed: 11241712]

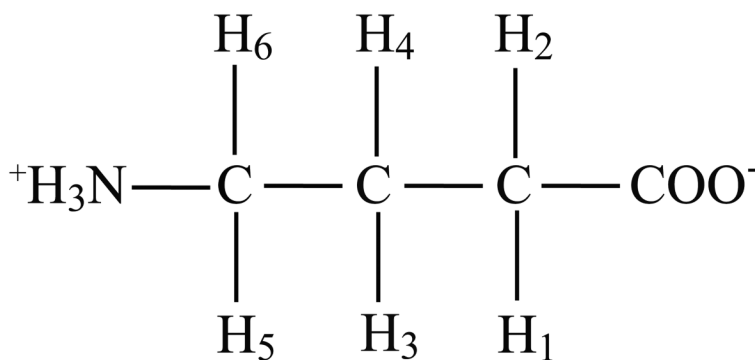


Figure 1. Chemical formula of GABA. Proton indices correspond to those listed in Table I.

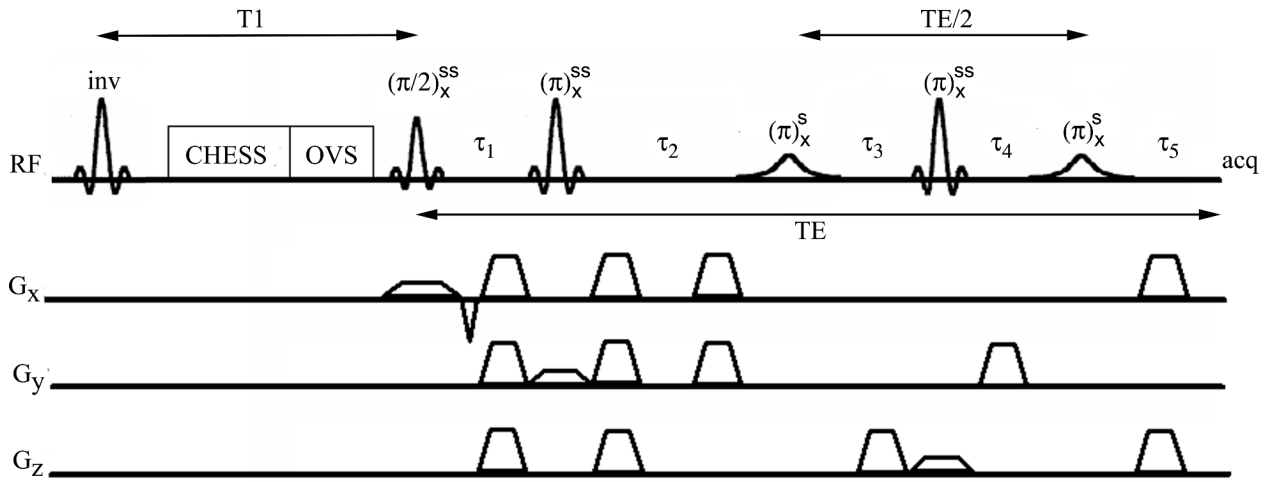


Figure 2. MEGA-PRESS J-difference editing pulse sequence with T1 nulling, CHES water suppression, and outer volume suppression.

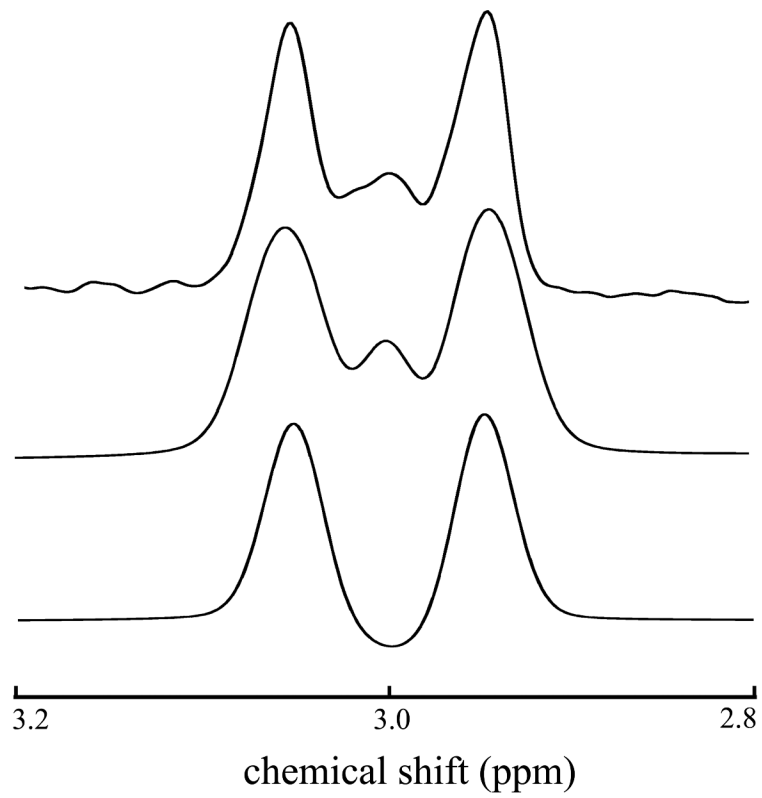


Figure 3. In-vitro (top) and simulated GABA edited spectra. The middle and bottom traces result from simulating GABA as an AA'XX'WW' versus an $A_2X_2W_2$ spin-system, respectively.

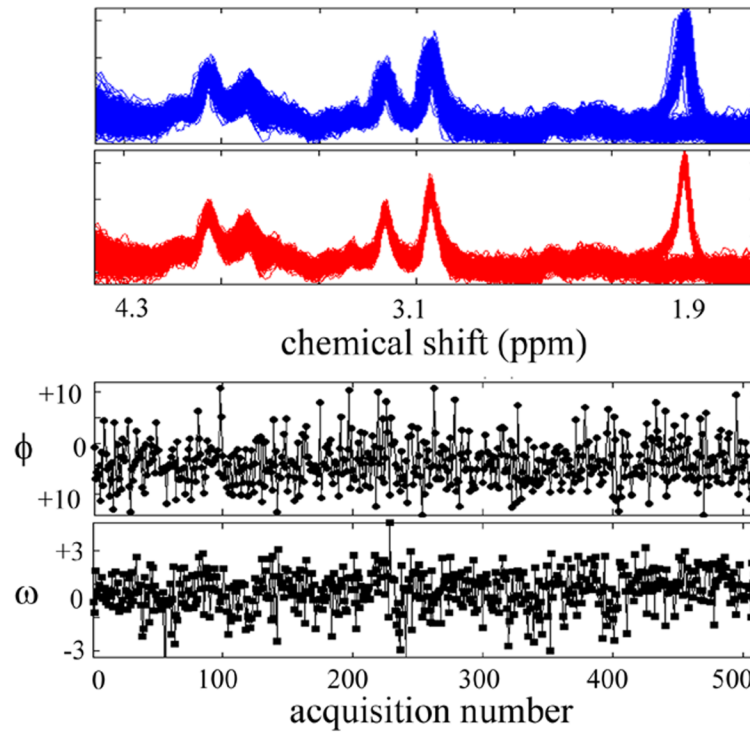


Figure 4. From bottom to top, frequency (ω) and phase (ϕ) variations as a function of acquisition number, respectively, and corrected (red) and raw (blue) data for a typical in-vivo acquisition from a 22.5 mL voxel containing mostly frontal grey matter.

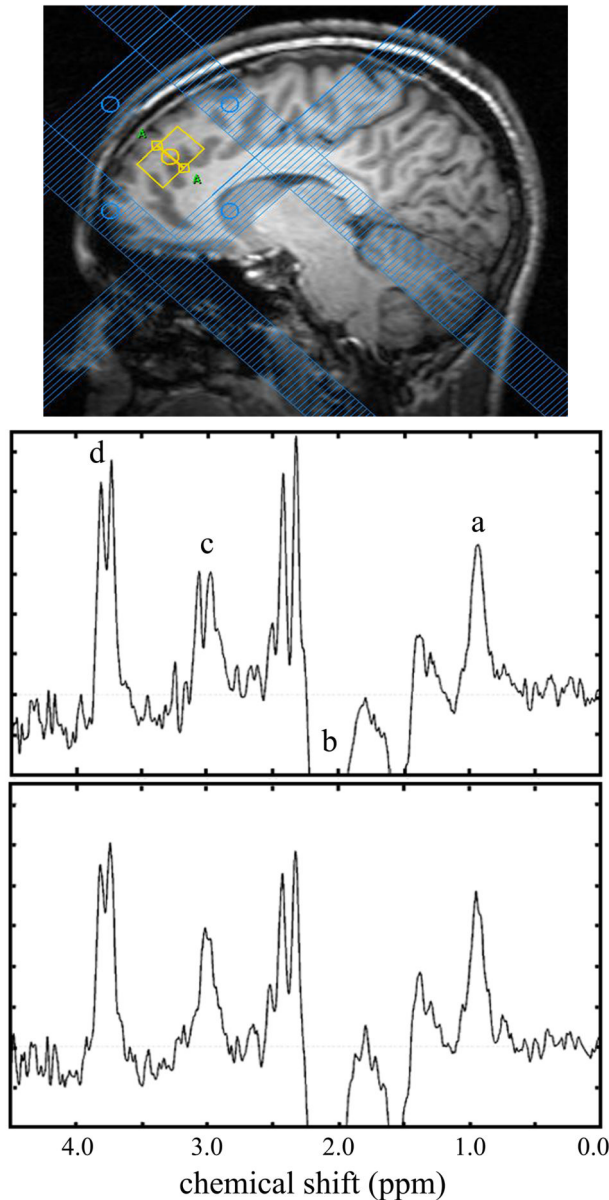


Figure 5. In-vivo GABA*-edited data acquired from a 22.5 mL anterior cingulate grey matter voxel (256 transients, 2.5 s recycle delay, 4 Hz exponential broadening, 2k samples, 2 kHz spectral width) with (top) and without (bottom) retrospective frequency and phase correction plotted with identical intensity axes. Peaks labeled a-d correspond to co-edited macromolecules, N-acetylaspartate, GABA, and a combination of co-edited glutamate, glutamine and glutathione, respectively.

Table I

Chemical shifts and coupling constants for GABA.

Resonance	Chemical Shift (ppm) ^{1,2}	J-coupling (Hz) ^{2,3}
H1	3.0128	H1-H3 (5.37), H1-H4 (7.13)
H2	3.0128	H2-H3 (10.58), H2-H4 (6.98)
H3	1.8890	H3-H5 (7.76), H3-H6 (7.43)
H4	1.8890	H4-H5 (6.17), H4-H6 (7.93)
H5	2.2840	
H6	2.2840	

¹ relative to ¹H₂O (4.65 ppm).

² chemical shifts and coupling constants taken from ref 9.

³ redundant couplings not listed ($J_{ij} = J_{ji}$).

Table II

Intensity ratios of GABA to other brain metabolites acquired from difference editing (n=20) in frontal lobe voxels (26.12 +/- 6.25 mL) containing mostly grey matter.

	Creatine	Gsx¹	Choline	NAA²
Ratio	0.055 (0.011)	0.62 (0.14)	0.080 (0.016)	0.041 (0.011)

¹ Glx and glutathione co-edited signal at ~3.7 ppm.

² measured from even acquisitions (selective inversion "off") and doubled.